CHEMICAL ENGINEERING TRANSACTIONS
VOL. 41, 2014
A publication of AIDIC
The Italian Association of Chemical Engineering
www.aidic.it/cet
Guest Editors: Simonetta Palmas, Michele Mascia, Annalisa Vacca
Copyright © 2014, AIDIC Servizi S.r.l.,
ISBN 978-88-95608-32-7; **ISSN** 2283-9216
DOI: 10.3303/CET1441015

Modeling of Through-Mask Electrochemical Micromachining

Alexey D. Davydov*[a], Tatyana B. Kabanova[a], Vladimir M. Volgin[a,b]

[a]Frumkin Institute of Physical Chemistry and Electrochemistry, Russian Academy of Sciences, Leninskii pr. 31, Moscow 119071, Russia
[b]Tula State University, pr. Lenina 92, Tula 300012, Russia
davydov@elchem.ac.ru

The through-mask electrochemical machining of features of micron dimensions was studied theoretically. The Laplace equations for the electric field potential and the equation of workpiece surface evolution were used as the mathematical model of the process. The problem was solved numerically using the methods of finite and boundary elements, and also the “Level Set” method. By using the numerical experiments, the effect of parameters, which characterize the mask geometry and the process conditions, on the initial distribution of current density over the workpiece surface and the variation of current distribution in the course of etching was studied. In particular, the dependences of dimensionless average current density on a fraction of unprotected areas were obtained at various values of mask thickness and unprotected areas (rectangular grooves or circles).
It is shown that the higher is the unprotected area density, the mask thickness, and unprotected area width, the higher is the initial average current density.
It is shown that the initial nonuniformity of average current density changes in the course of machining leading to a change in a ratio between the anodic dissolution rates of unprotected areas of different widths. In the initial period of treatment, the smaller is the width of uncovered area, the higher is the anodic dissolution rate. Then, in the course of machining, the anodic dissolution rate on the narrow unprotected areas steeply decreases and can become lower than that on the wider areas. As a result, the depth of unprotected areas of different sizes will be different. The result of modeling enables one to predict the final depth of the features on the workpiece surface.

1. Introduction

The through-mask electrochemical machining is one of effective methods of microfabrication (Datta, 1998), which is used to fabricate precision nozzles (Datta, 1995), regular relifs (Volgin and Davydov, 2004), complex patterned substrates (Raffelstetter and Mollay, 2010), micro-dimples arrays (Qian et al., 2010), micro probe arrays (Kim et al., 2011), etc. This method enables one to machine not only bulk metal (Kern et al., 2007), but also thin metal films (West et al., 1992). Various combinations of template anodic dissolution and cathodic electrodeposition (Herraiz-Cardona et al., 2013) can be used for production of highly porous metal layers and complex hierarchical patterns.
The shape and dimensions of a workpiece, which is fabricated by the through-mask electrochemical machining depend on a large number of parameters: the mask thickness, shape and dimensions of unprotected areas (West et al., 1992), mask wall angle (Li et. al, 2011), the machining mode and conditions of mass transfer (Alkire and Deligianni, 1988), etc. Therefore, the process of electrochemical machining is frequently studied by the theoretical methods (Davydov et al., 2004). The theoretical study of the process is commonly performed using the mathematical models, which involve the Laplace equation for the electric field potential (Shenoy et al., 1996) or concentration of dissolving metal ions (Madore et al., 1999). The regularities of electrochemical shaping of individual elements have been much studied (Li et al., 2010). The results of these studies enabled one to estimate the effect of hydrodynamics of electrolyte solution flow; to predict the formation of metal “islands” on the substrate and develop the methods, which provide the absence of the islands; to take into account the effect of the incline of side mask walls on the geometry of machined surface, etc. Frequently, a mask has the blanks of different shapes and dimensions.

Please cite this article as: Davydov A., Kabanova T., Volgin V., 2014, Modeling of through-mask electrochemical micromachining, Chemical Engineering Transactions, 41, 85-90 DOI: 10.3303/CET1441015

In this case, it is important to take into consideration a mutual effect of mask elements (Raffelstetter and Mollay, 2010). By now, the regularities of electrochemical machining of micro features using the masks with the elements of different shapes and sizes have not been studied adequately.
The aim of this work is to study theoretically the regularities of mask electrochemical machining on the basis of recent achievements in the field of modeling of electrochemical machining (Hinduja and Kunieda, 2013).

2. Statement of problem

In the general case, the mask can have the blanks of different shapes (for example, grooves, circles, etc.) and sizes, and they are nonuniformly arranged over the workpiece surface (Figure 1). A dependence of the current density and, consequently, the rate of metal anodic dissolution, on the protected surface area leads to the formation of elements of different depth on the workpiece surface areas with different geometric parameters. For instance, in zone I, where a fraction of unprotected surface area is smaller than in zone II, the resulting relief elements will be deeper than that in zone II (Figure 1). In addition, due to the screening effect, the depth of the elements will differ also within each zone. For instance, in zone I, the element of relief with a larger fraction of unprotected area (4) will be deeper than that with smaller unprotected area (3). At equal characteristic sizes of mask elements of different geometric shapes (b = D, where b is the width of the groove-shaped unprotected area (5) and D is the diameter of the round unprotected area (6)), the machining will yield the elements of different depth (Figure 1, zone III, (5) and (6)): due to a larger contribution of the edge effect, the axisymmetric element will be deeper than the straight-line groove.

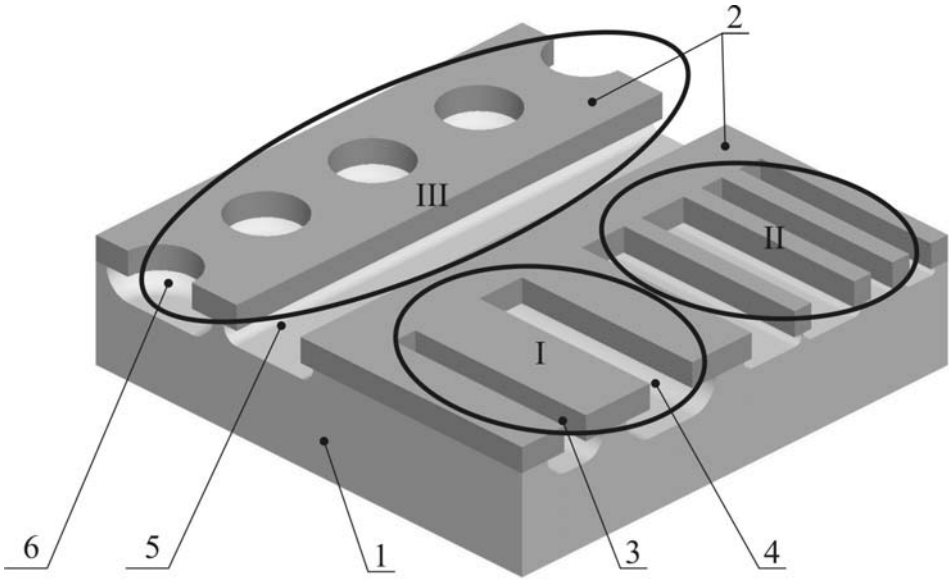

Figure 1: A scheme of electrochemical machining using the mask with the blanks of different shapes and sizes: (1) a workpiece (substrate); (2) a mask

As a rule, several elements with various shapes and sizes should be formed on the workpiece surface. Due to the overcutting and edge effects, the sizes of elements and the rates of their formation will be different. In order to predict the workpiece surface geometry, and also to determine the shape and sizes of mask elements, which is required to produce the prescribed workpiece surface geometry, it is advantageous to apply the methods of mathematic modeling.

3. Mathematical model and method of numerical solution

The electrochemical machining with partial insulation of workpiece surface is simulated by the model of shaping, which ignores the concentration changes in the solution (Davydov et al., 2004). This approximation is acceptable in the cases of sufficiently intense pumping or stirring of electrolyte solution. The distribution of electric potential over the interelectrode gap is calculated by using the Laplace equation.

For convenience of solution and analysis of the results, the mathematical model is given in the dimensionless form. The interelectrode gap (*S*) was taken as a unit length, and the applied voltage (*U*) was taken as a unit electric potential.

$$X = \frac{x}{S},\ Y_a = \frac{y_a}{S},\ \Phi = \frac{\varphi}{U},\ I = \frac{S}{\chi U} i,\ \ \tau = \frac{\eta \varepsilon_V \chi U}{S^2} t \tag{1}$$

where X, Y_a are the dimensionless coordinates; Φ is the dimensionless potential; I is the dimensionless current density; τ is the dimensionless time; η is the current efficiency; ε_V is the volumetric electrochemical equivalent; χ is the conductivity of electrolyte solution; *a* is the subscript, which characterizes the workpiece surface.
Thus obtained system of dimensionless equations is as follows:

$$\operatorname{div}(\operatorname{grad}\Phi) = 0 \tag{2}$$

$$\frac{\partial Y_a}{\partial \tau} = \frac{\partial \Phi}{\partial n}\sqrt{1+\left(\frac{\partial Y_a}{\partial X}\right)^2} \tag{3}$$

where *n* is a vector normal to the workpiece surface.
To solve the system of Eqs. (2) and (3), the boundary and initial conditions should be prescribed. For the machining scheme under consideration, when the polarization of electrodes can be ignored, the boundary conditions for the dimensionless potential will be as follows:

$$\Phi = \begin{cases} 1, \text{ on the anode (workpiece)} \\ 0, \text{ on the cathode (tool - electrode)} \end{cases}$$
$$\frac{\partial \Phi}{\partial n} = 0, \text{ on the insulator} \tag{4}$$

The initial condition is that, at the initial instant of time, the workpiece surface is a plane passing through the origin of coordinates:

$$Y_a(0) = 0 \tag{5}$$

The boundary value problem for Eqs. (2) – (5) is a problem with moving boundary. Then, the equations, which describe the transport processes and the motion of computational region boundary, should be calculated simultaneously. This presents a considerable difficulty. The numerical solution is frequently simplified by using the quasi-steady state approximation. Within this approximation, the entire time of machining was divided into a number of time steps. For each time step:
1) the distribution of electric potential was calculated (at the electrode geometry corresponding to the beginning of the step);
2) a new shape of the workpiece surface was determined (at the distribution of the current density corresponding to the beginning of the step).
At each time step, the boundary-value problem for the Laplace Eq. (2) with the boundary conditions (4) was solved numerically by the method of boundary elements. The boundary-value problem was reduced to the equivalent boundary integral equation. As a result of numerical solution of Eq. (2), the distribution of the current density over the workpiece surface was determined. It was used to solve Eq. (3) and determine the geometry of workpiece surface for the next time step.

4. Results of modeling and discussion

At the first stage, the initial stage of electrochemical machining with partial insulation of workpiece surface was simulated, i.e. the distribution of dimensionless current density (anodic dissolution rate) over the workpiece surface was calculated. The calculations were performed at various values of machining parameters, such as the blank width, mask thickness, a fraction of active workpiece surface area, i.e. a ratio of unprotected area to the total surface area of the workpiece. Based on these results, the general regularities for a mask with active areas of identical shapes and sizes can be formulated as follows: An

average current density monotonically decreases with decreasing distance between the mask elements (increasing active surface area) and increasing mask thickness. An average current density for the axisymmetric (circle) unprotected areas is higher than that for the linear (band, strip) unprotected areas.
In the majority of cases of practical importance, the masks have active areas of different sizes. In this case, the rates of formation of different elements will differ; as a result, the elements of different depth will form on the workpiece surface. A difference between the element depths can be estimated by using the above regularities for the uniform mask. However, it is difficult to determine an actual active surface area.

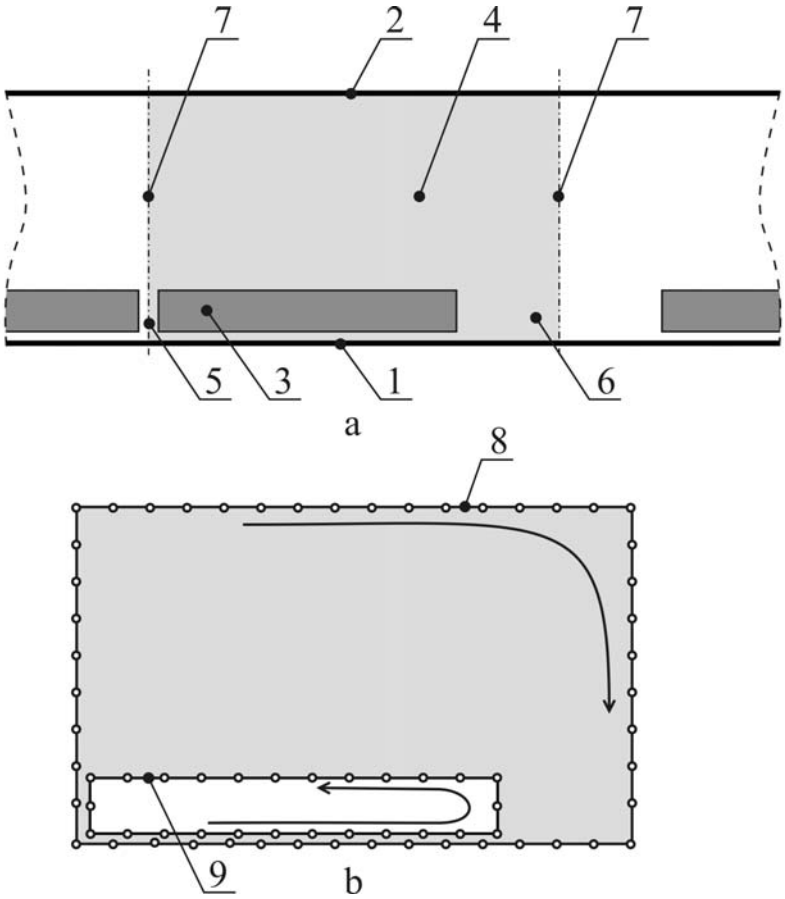

Figure 2: A fragment of zone of electrochemical machining and (b) computational region

At the second stage, the electrochemical machining using the masks with active areas of two different sizes was performed. Figure 2 (a) gives a fragment of zone of electrochemical machining with (1) the anode, (2) the cathode, and (3) the mask. The interelectrode gap (4) is filled with the electrolyte solution. The mask contains the blanks (5), (6) of different width. The planes of symmetry that bound the computational region are denoted by 7. Figure 2b gives the computational region. The computational nodes (Figure 2b) are shown with circles; the arrows show the direction of numbering the computational nodes on the outer boundary (8) (corresponds to Figure 2a, lines 1, 2, and 7) and inner (mask/electrolyte) boundary (9). For convenience of modeling, it was assumed that there is a small gap between the initial workpiece surface and the mask. The presence of the gap of the order of 0.001 to 0.1 had no considerable effect on the results of modeling; however, it enabled us to simplify significantly the algorithm of calculations due to the presence of two different surfaces (the workpiece surface and the mask surface).
To provide the required accuracy of simulation at the minimum amount of computation, a nonuniform mesh of boundary elements was used. To maintain the accuracy in the course of surface evolution, the adaptive remeshing was realized. As it was found by the test calculations, a time step of 0.001 and shorter provided the stability of numerical simulation. In addition, a “Level Set” method was used for discretization of spatial derivative in equation (3):

$$Y_{a,i}^{n+1} = Y_{a,i}^{n} + \Delta\tau \left.\frac{\partial \Phi^{n}}{\partial n}\right|_{i} \sqrt{1 + \left[\max\left(\frac{Y_{a,i+1}^{n} - Y_{a,i}^{n}}{X_{i+1} - X_{i}}, 0\right)\right]^{2} + \left[\min\left(\frac{Y_{a,i}^{n} - Y_{a,i-1}^{n}}{X_{i} - X_{i-1}}, 0\right)\right]^{2}} \quad (6)$$

where *i* is the number of computational node on the workpiece surface; *n* is the number of time step; and $\Delta\tau$ is the time step.

Figure 3 gives the results of modeling for a mask of dimensionless thickness (a) and (c) $\bar{h} = 0.1$; (b) and (d) $\bar{h} = 0.01$; the dimensionless sizes of blanks are $\bar{b} = 0.1$ (on the left) and $\bar{b} = 1$ (on the right); (a) and (b) a fraction of active surface area is 27.5 %; (c) and (d) a fraction of active surface area is 55 %. Dashed lines show the workpiece surface at the time, when the elements on different unprotected areas reach equal depth.

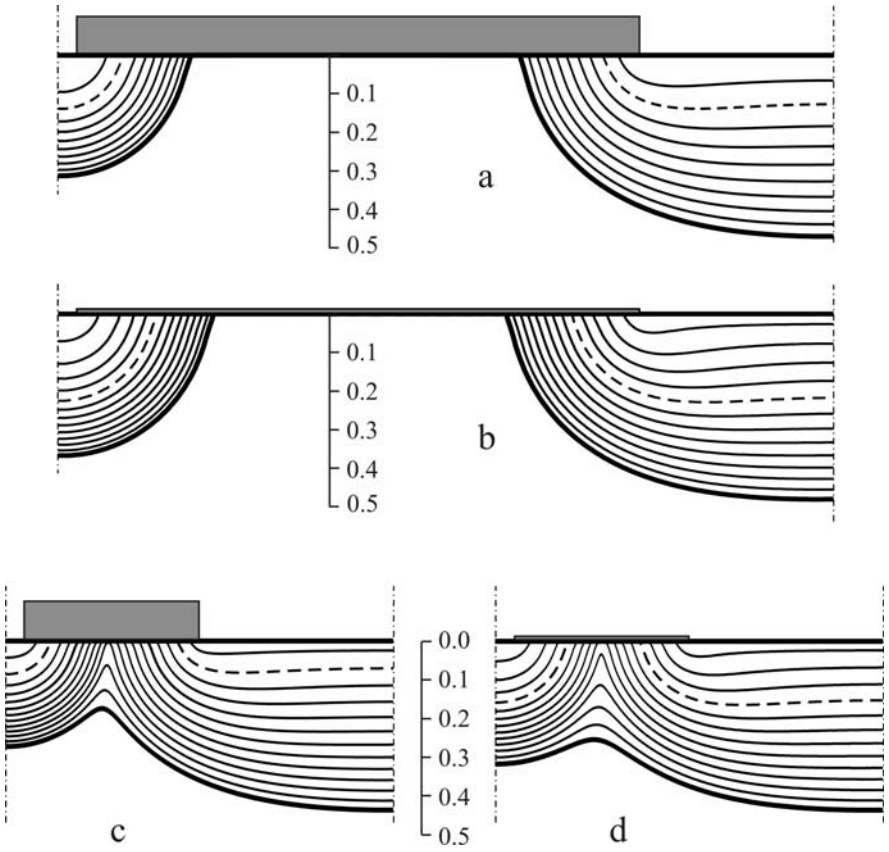

Figure 3: Workpiece surface evolution in the electrochemical machining using a mask with active areas of 0.1 (the left parts of the figures) and 1 (the right parts of the figures)

From Figure 3, it is seen that, in the initial period of machining, a higher rate of anodic dissolution is observed on smaller active areas. As a result of machining, the active workpiece surface area increases. At a constant current, this leads to a decrease in the current density and, consequently, the anodic dissolution rate.

To the first approximation, assume that the anodic dissolution is isotropic and the current through a blank is constant. Then,

$$\frac{dY_a}{d\tau} = \frac{\bar{b}}{\bar{b} + \pi Y_a} I_{\text{av}} \quad (7)$$

where I_{av} is dimensionless average current density.

From (7), it follows that the anodic dissolution rate decreases faster on the smaller unprotected areas.

Thus, in the course of machining, a ratio between the anodic dissolution rates in different blanks permanently varies. Under certain conditions, the anodic dissolution rate on the larger unprotected areas becomes higher than that on the smaller unprotected areas.
At a shorter time of machining, the elements with narrower unprotected areas will be deeper, whereas at a longer time, the elements with wider unprotected areas will be deeper. The time (or depth), when equal depth of different elements is reached, depends on the mask thickness and a fraction of active surface area (Figure 3).

5. Conclusions

A scheme of numerical modeling of through-mask electrochemical machining, which enables one to predict the shape and sizes of workpiece surface, is developed. The developed mathematic model enables one to determine the time dependence of unprotected area depth and to determine the treatment time, which is required to obtain equal depth for the areas of different sizes.

Acknowledgements

This work was supported by the Russian Foundation for Basic Research, project no. 13-03-00537 and the Ministry of Education and Science of the Russian Federation, project no. 1096 of the Basic Part of the State Program.

References

Alkire R., Deligianni H., 1988, The Role of mass transport on anisotropic electrochemical pattern etching, Journal of The Electrochemical Society 135, 1093-1100.

Datta M., 1995, Fabrication of an array of precision nozzles by through-mask electrochemical micromachining, Journal of The Electrochemical Society 142, 3801-3805.

Datta M., 1998, Microfabrication by electrochemical metal removal, IBM Journal of Research and Development 42(5), 655-669.

Davydov A.D., Volgin V.M., Lyubimov V.V., 2004, Electrochemical machining of metals: Fundamentals of electrochemical shaping, Russian Journal of Electrochemistry 40, 1230-1265.

Herraiz-Cardona I., Gonzalez-Buch C., Ortega E., Garcia-Anton J., Perez-Herranz V., 2013, Energy efficiency improvement of alkaline water electrolysis by using 3D Ni cathodes fabricated via a double-template electrochemical process, Chemical Engineering Transactions 32, 451-456.

Hinduja S., Kunieda M., 2013, Modelling of ECM and EDM processes, CIRP Annals - Manufacturing Technology 62(2), 775-797.

Kern P., Veh J., Michler J., 2007, New developments in through-mask electrochemical micromachining of titanium, Journal of Micromechanics and Microengineering 17, 1168-1177.

Kim Y., Youn S., Cho Y.-H., Park H., Chang B.G., Oh Y.S., 2011, A multi-step electrochemical etching process for a three-dimensional micro probe array, Journal of Micromechanics and Microengineering 21, Art. No. 015019.

Li W., Quandai W., Xiuqing H., Yucheng D., Bingheng L., 2010, Finite element simulation and experimental study on the through-mask electrochemical micromachining (EMM) process, International Journal of Advanced Manufacturing Technology 51, 155-162.

Li D., Zhu D., Li H., Liu J.-G., 2011, Effects of mask wall angle on matrix-hole shape changes during electrochemical machining by mask, Journal of Central South University of Technology 18, 1115-1120.

Madore C., Piotrowski O., Landolt D., 1999, Through-mask electrochemical micromachining of titanium, Journal of The Electrochemical Society 146, 2526-2532.

Qian Sh., Zhu D., Qu N., Li H., Yan D., 2010, Generating micro-dimples array on the hard chrome-coated surface by modified through mask electrochemical micromachining, International Journal of Advanced Manufacturing Technology 47, 1121-1127.

Raffelstetter P., Mollay B., 2010, On the modeling of shape evolution in through-mask electrochemical micromachining of complex patterned substrates, Electrochimica Acta 55, 2149-2157.

Shenoy R.V., Datta M., Romankiw L.T., 1996, Investigation of island formation during through-mask electrochemical micromachining, Journal of The Electrochemical Society 143, 2305-2309.

Volgin V.M., Davydov A.D., 2004, Modeling of multistage electrochemical shaping, Journal of Materials Processing Technology 149(1-3), 466-471.

West A.C., Madore C., Matlosz M., Landolt D., 1992, Shape changes during through-mask electrochemical micromachining of thin metal films, Journal of The Electrochemical Society 139, 499-506.